Fibers and Polymers 2020, Vol.21, No.9, 1983-1991
DOI 10.1007/s12221-020-9461-3

ISSN 1229-9197 (print version)
ISSN 1875-0052 (electronic version)

Novel One Step Printing and Functional Finishing of Wool Fabric Using Selenium Nanoparticles

Tarek Abou Elmaaty[1]*, Sally Raouf[1], and Khaled Sayed-Ahmed[2]

[1]*Faculty of Applied Arts, Damietta University, Damietta 34512, Egypt*
[2]*Faculty of Agriculture, Damietta University, Damietta 34512, Egypt*

(Received May 7, 2019; Revised September 18, 2019; Accepted December 20, 2019)

Abstract: This study demonstrates the possibility of one step printing and multifunctional finishing of wool fabrics using synthesized selenium nanoparticles (Se-NPs) as stable functional colorant. Se-NPs formation was emphasized using visible changes, UV-visible absorption spectra, and transmission electron microscopy (TEM) analysis. The UV-visible spectra and TEM analysis confirmed the synthesis of spherical well-dispersed Se-NPs. The examination of printed samples was conducted by scanning electron microscopy (SEM), energy dispersive X-ray spectroscopy (EDX), and X-ray powder diffraction analysis (XRD), that revealed the successful deposition of Se-NPs onto wool fabric surface. The color, UV protection, and antimicrobial properties of Se-NPs printed wool were also evaluated. The printed samples had outstanding fastness characteristics to washing, rubbing, and light. Moreover, Se-NPs printed samples were found to possess outstanding antimicrobial activities, excellent UV-protection properties with a remarkable durability after 10 washing times without any negative impact on the printing and softness characteristics.

Keywords: Multifunctional printing, Wool fabrics, Se nanoparticles, Antimicrobial, UV protection

Introduction

Printing is a world-renowned process in textile industry, which is known as a conventional textile-finishing procedure in which dyes or pigments are applied onto a fabric surfaces. Moreover, printing can be performed with various dyes or pigments and several techniques. The most commonly used printing technique is screen printing which is characterized by simplicity, versatility, low cost, and applicability to almost every kind of textiles [1,2].

Wool as a natural fiber has unique chemical and physical properties that made the fiber be extremely versatile. Wool fabrics are highly praised by consumers because of their excellent comfort properties during wearing [3]. Some studies have been accounted for printing wool fabrics with acid dyes [4] and reactive dyes [5,6] that have better solubility than acid dyes. However, the reactive dyes used in printing often have only 60 % degree of fixation [7]. Because of cytotoxicity problems of other synthetic dyes, printing wool with natural dyes has been mentioned by many studies to give a range of high-fashion coloristic effect with antimicrobial properties [8,9]. However, despite being eco-friendly, natural dyes is found to yield poor color and inadequate fastness properties [10]. Furthermore, printing fabrics with dyes or pigments requires the presence of catalyst, handle modifier, cross-linker, surfactant, and other auxiliaries that may have toxic impacts to human and environment. In addition, allergy, toxic effects, and low fastness properties of some synthetic and natural dyes have been reported [11] and consequently initiated the need for decreasing the environmental effects of the printing process as well as enhancing the properties of printed materials.

Recently, prominent possibilities of nanoparticles (NPs) can be effectively applied for producing textiles with multi-functionalities. A number of studies have been made for imparting functionalities to different textiles, such as antimicrobial, UV-blocking, and self-cleaning properties [12-15], as well as many approaches were interested in their preparation and characterization, as each of the NPs has different colors indicated by their surface plasmon resonance (SPR) peaks [16]. Lately, new approaches for applying NPs as multifunctional agent imparting coloration, antimicrobial, and UV protection properties using silver, cupric, silica, and gold NPs for wool fabrics [17-19], nylon [20], cotton, and polyester [21,22] have been reported.

Selenium nanoparticle (Se-NP) with a bright red color has become the new research target, because it exhibits low toxicity compared to selenium compounds and have excellent bioactivities [23]. Some studies also investigated the antimicrobial properties of synthesized Se-NP and its potential biological application as anticancer agent [24-27]. Its surface plasmon resonance (SPR) property in textile coloration and its functional properties in textiles have not been reported yet.

Accordingly, the main task of this work was to introduce for the first time a cost-effective eco-friendly approach by harnessing the SPR effects of Se-NPs to develop new functionalized printed wool fabrics with a range of colors in a single step.

Experimental

Materials

Bleached wool fabrics (100 % scoured) were utilized.

*Corresponding author: tasaid@du.edu.eg

Sodium alginate (sodium polymannuronate, $C_6H_7O_6Na$, ex-pure), Urea (ex-pure), and acetic acid were purchased from Oxford Lab Chem, India. Sodium hydrogen selenite, ascorbic acid, and PVP (polyvinylpyrrolidone) were purchased from Loba Chemie, India. The all of other chemicals used during work were of commercial grade.

Methods

Preparation of Selenium Nanoparticles (Se-NPs)

Se-NPs were prepared through redox reaction according to the method described by Malhotra *et al.* with an improved modification [28]. Sodium hydrogen selenite was utilized as a precursor for Se-NPs with different concentrations (10-100 mM). It was added to vitamin C at various concentrations (10-100 mM) in the ratio of 1:1 and at the same concentration under magnetic stirring. Se-NPs stability was maintained using PVP (polyvinylpyrrolidone) dissolved in vitamin C solution (0.3-3 g/100 m*l*). The color converted from colorless to dark orange [28].

Printing Paste Method

The Se-NPs printing paste was prepared according to the formulation as shown in Table 1.

The homogenized Se-NPs based printing paste was applied to wool fabrics using screen printing technique, then the printed samples were fixed at 98 °C for 6 min, finally samples were washed off with non-ionic detergent at 60 °C for 10 min and material-to liquor ratio at 1:50.

Characterization

The morphology and particle size of the prepared Se-NPs were evaluated by transmission electron microscope (TEM) using a JEM 2100F electron microscope (JEOL, Japan) at 200 kV.

The UV-Vis absorption spectra of Se-NPs solutions were obtained using a Shimadzu UV-1800 UV-visible spectrophotometer (Shimadzu Co., Japan).

Surface morphology of blank and Se-NPs printed wool fabrics was observed using a JEOL JSM-6510LB (Japan-Tokyo) with energy dispersive spectrum (EDX) analysis.

The crystal behavior of prepared Se-NPs and printed samples was obtained using an X-ray diffractometer (Bruker D8 ADVANCE, Karlsruhe, Germany). Se-NPs solution was dried at 130 °C until completely dryness for XRD analysis.

Table 1. Se-NPs based printing formulation

Printing paste components	g/kg paste
Sodium alginate (15 %)	500
Urea	70
Acetic acid (30 %)	50
Se nanomaterial	20
Water	360
Total	1000

X-ray photoelectron spectroscopy (XPS) analysis for Se-NPs printed sample was conducted using a high-resolution photoelectron spectrograph (Escalab 250Xi; Thermo Fisher Scientific). Energy resolution (0.05 eV) and dualbeam charge neutralization system consisting of a low-energy electron flood gun (~1 eV) and an Argon ion gun (≤ 10 eV) were utilized.

Functional Properties of Se-NPs Printed Fabrics

The functionalities of Se-NPs printed wool samples were evaluated in terms of antimicrobial activity and UV protection factor (UPF).

Antimicrobial Activity

Antimicrobial activity of printed wool samples was tested against G+ve bacteria (*Bacillus cereus* & *Staphylococcus aureus*) in addition to G-ve bacteria (*Escherichia coli*) & Yeast (*Candida utilis*). The antimicrobial tests were performed quantitatively using the standard test method in accordance with AATCC Test Method (147-2004) [29], and expressed as zone of growth inhibition (mm).

UV-Protection Properties

The ultraviolet protection factor (UPF) and UV-blocking activities of printed wool samples were evaluated using AS/NZS 4399:1996 test method, and protection was rated as good, very good, or excellent, if their UPF values range from 15 to 24, 25 to 39, or on top of 40, respectively.

Testing

Se-NPs cytotoxicity was evaluated on human normal melanocyte cell line (HFB_4) using MTT assay [30]. 96 well plate of tissue culture was inoculated with 1×10^5 cells/m*l* (100 µ*l*/well) and incubated at 37 °C for 24 h. Then, medium decantation from 96 well plates was conducted after cells confluent sheet formation. The monolayer of cells was washed twice using wash media. Two-fold dilutions of each sample were prepared in RPMI medium utilizing 2 % serum (maintenance medium). Moreover, 0.1 m*l* of every dilution was checked in different wells in addition to 3 wells as a control, containing just maintenance medium. At this point, plate was kept at 37 °C and examined to observe the cytotoxicity physical signs. MTT solution (5 mg/m*l*) was prepared in PBS. Additionally, 20 µ*l* MTT were added to every well with shaking for 5 min at 150 rpm. Then, wells were incubated with *aeration* of 5 % CO_2 at 37 °C for 4 h to metabolize MTT. Formazan, the product of MTT metabolism, was resuspended in 200 µ*l* DMSO with shaking (5 min at 150 rpm). Finally, optical density was read at 560 nm and 620 nm after subtracting background.

The L^* (lightness), a^* (redness-greenness), b^* (yellowness-blueness), C^* (Chroma), h (hue) color coordinates and color strength (K/S) of the Se-NPs printed wool fabrics were assessed by a spectrophotometer (CM-3600d, Konica Minolta, Japan).

The washing, rubbing, and light color fastnesses of Se-

NPs printed wool fabrics were carried out according to the standard AATCC Test Methods (61-2009) [31], (8-2007) [32], and (16-2004) [33], respectively.

Durability to washing was assessed by AATCC Standard Test Method 61(2A)-2009 [34] after 10 laundering cycles.

Results and Discussion

Characterization of Synthesized Se-NPs

TEM Analysis

Se-NPs formation was confirmed by TEM analysis. Figure 1 showed the morphology of prepared Se-NPs with different concentrations. The representative TEM images showed the formation of well-dispersed Se-NPs that were almost spherical in shape. As indicated by TEM analysis, Se-NPs at varied concentrations of 5, 12.5, 25, 37.5, and 50 mM had various diameters at the range of 40-120, 26-115, 16-108, 24-112, and 28-93 nm, respectively. Histogram bins were 20 nm wide while they centered at 25, 45, 65, 85, and 105 nm. All Se-NPs with diameters at the range of 35 nm and 55 nm were considered together as particles with size of 45 nm. The size of Se-NPs depended on PVP and sodium hydrogen selenite concentrations. Se-NPs at the concentrations of 25 and 50 mM had the lowest diameter as shown in Figure 2. Se-NPs at the concentration of 50 mM possessed the highest PVP content (3 g/100 m*l*) which consequently prevented any aggregation, whereas Se-NPs at the concentration of 5 mM showed the largest size (40-120 nm) in comparison with other formed Se-NPs due to their low PVP concentration (0.3 g/100 m*l*).

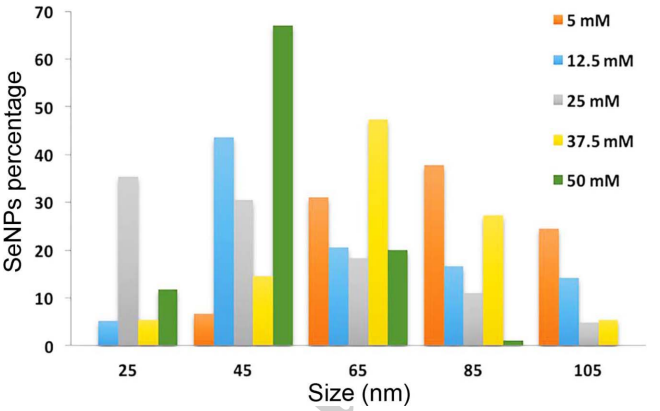

Figure 2. Histogram of size distributions of synthesized Se-NPs on different concentrations.

UV-Visible Spectra

Synthesis of Se-NPs was confirmed by UV-Vis spectra analysis by observing the color change from colorless to dark orange color (Se-NPs). The color change may be attributed to surface plasmon resonance phenomenon (SPR). The free electrons of metal nanoparticles are responsible for SPR absorption band, because of the electrons-combined vibration of metal nanoparticles. UV-Vis spectrophotometer was utilized for Se-NPs characterization at the range of 200

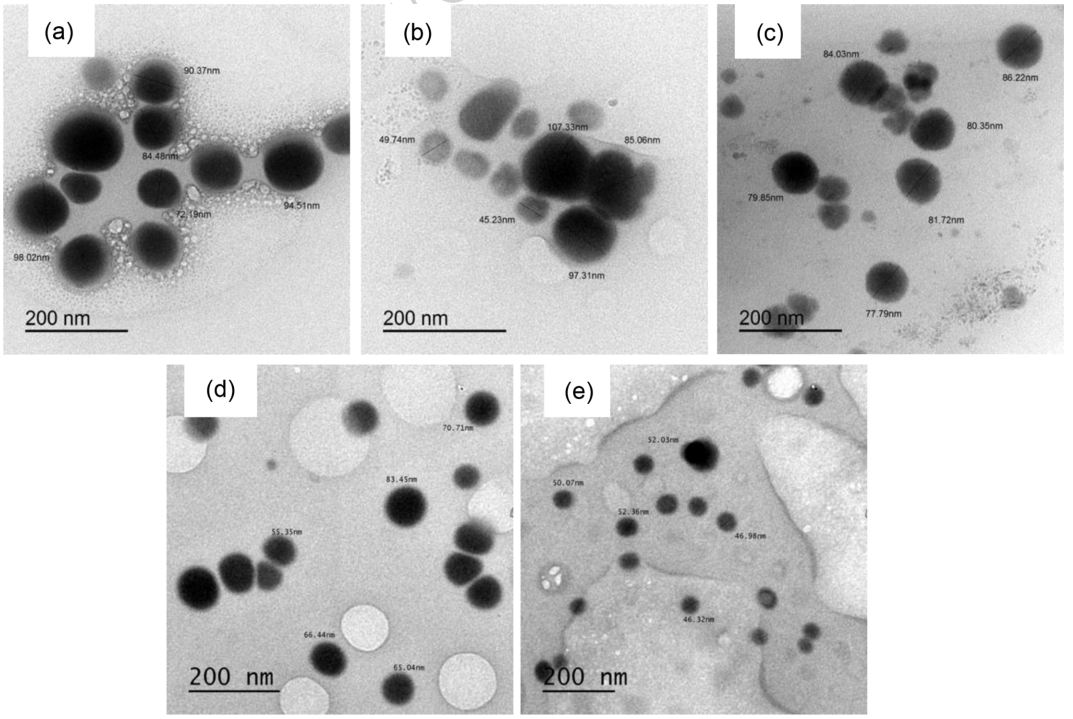

Figure 1. TEM images of synthesized Se-NPs on different concentration; (a) 5 mM, (b) 12.5 mM, (c) 25 mM, (d) 37.5 mM, and (e) 50 mM.

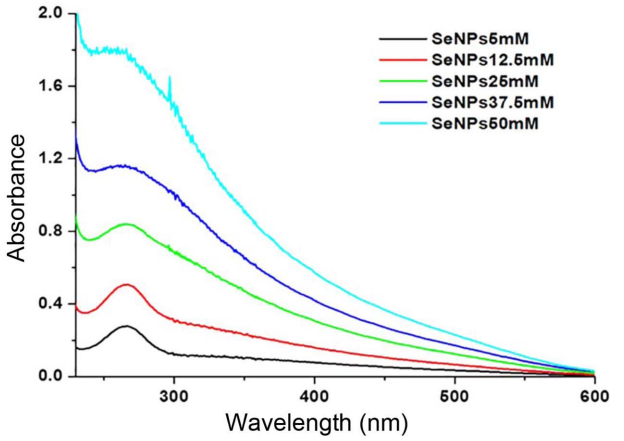

Figure 3. UV-visible spectrum of synthesized Se-NPs in different concentrations.

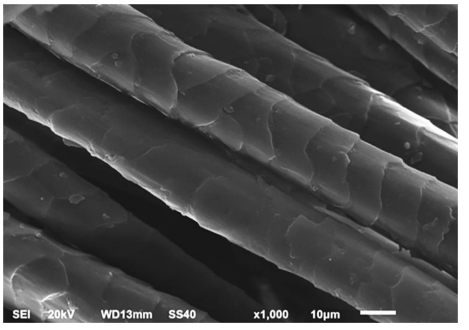

Figure 4. SEM images of blank wool fabric.

to 600 nm. The UV-Vis absorbance spectrum of prepared Se-NPs displayed a broad band at around 263 nm as shown in Figure 3, which confirmed the presence of spherical Se-NPs [35].

SEM and EDX Analysis

The surface morphologies of the blank and Se-NPs printed wool samples were given in Figures 4 and 5. SEM micrograph in Figure 4 exhibited a clean and smooth surface of blank wool fabric, whereas Figure 5 illustrated the SEM-EDX images of Se-NPs printed and functionalized samples. It was obvious that the fiber surface was coated by a sufficient layer of Selenium at the nanoscale, which confirmed the deposition of Se-NPs onto the surface of the printed samples. The EDX results and SEM images are strong evidence for the deposition of synthesized Se-NPs on the Se printed wool fabrics surface.

X-ray Diffraction (XRD)

X-ray powder diffraction is an efficient analytical technique used to further confirmation of Se-NPs crystal structure using monochromatic X-rays. The XRD patterns of synthesized Se-NPs and printed wool fabric were shown in Figure 6. The diffractions at 24.28 °, 29.24 °, and 43.64 ° can indicate the planes of (100), (101), and (102), respectively. These planes illustrated the presence of the face-centered cubic (fcc) of selenium. All the diffraction peaks showed good agreement with standard JCPDS data (card No. 06-0362). This clearly revealed the crystalline nature of prepared Se-NPs and very well corresponded to standard selenium powder [36].

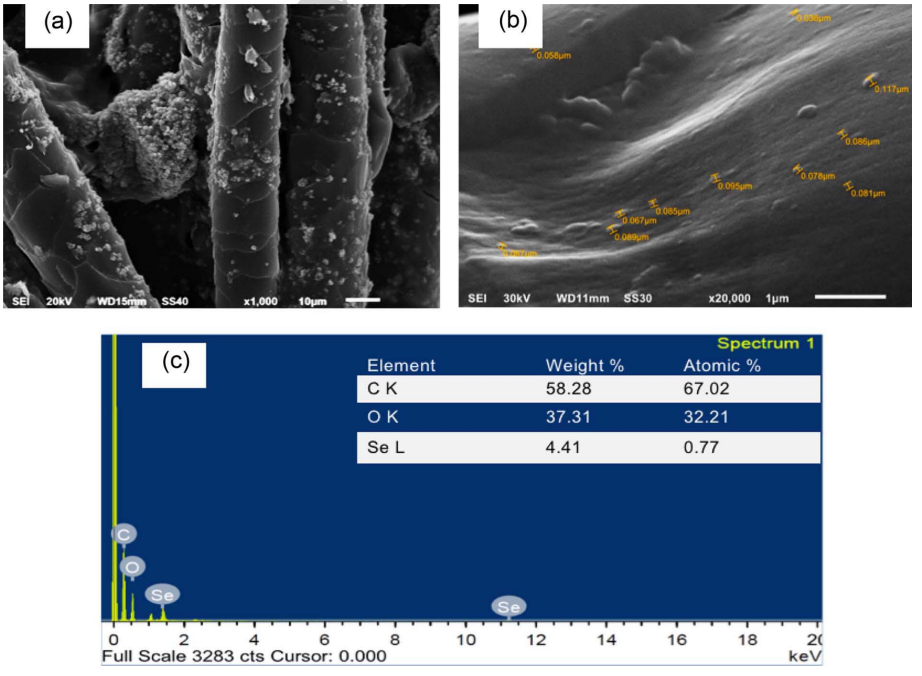

Figure 5. SEM images with magnification up to 1000 (a), 20.000 (b), and EDX spectrum (c) of Se-NPs printed wool fabric. K and L lines represented the orbitals in which the element is formed.

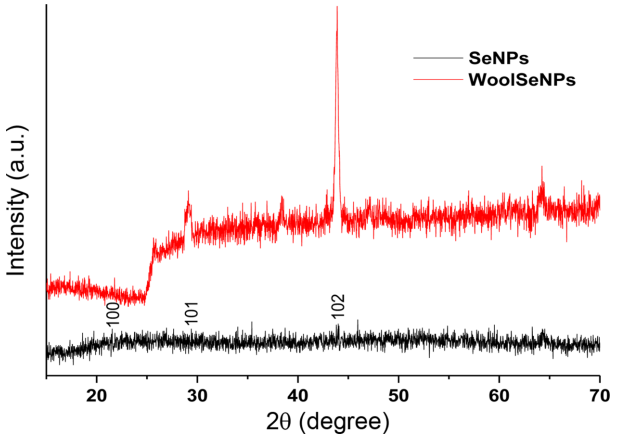

Figure 6. XRD patterns of Se-NPs and printed wool fabrics.

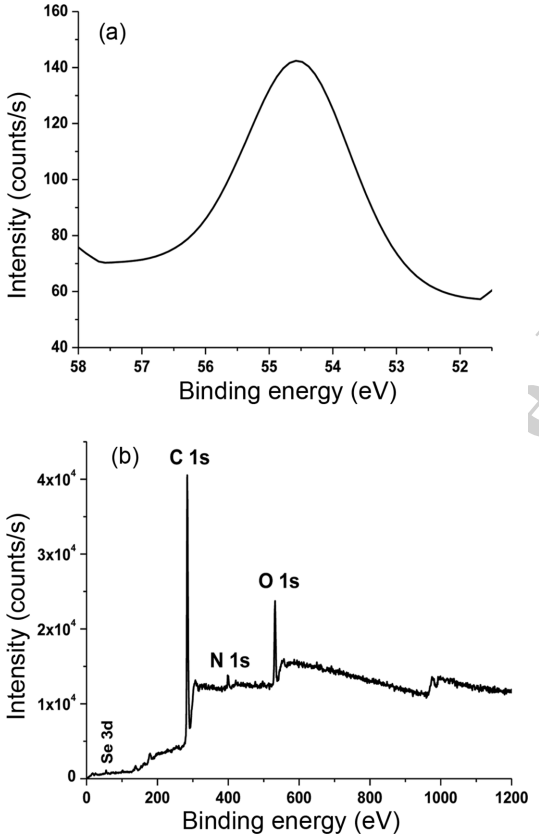

Figure 7. (a) Se 3d XPs pattern, (b) wide-range XPs pattern of Se-NPs, recorded by a high-resolution photoelectron spectrograph.

XPS Analysis

The successful introduction of Se-NPs on the surface of printed wool fabric was further confirmed by the XPS spectra and the result was shown in Figure 7. The XPS patterns of Se-NPs 3d orbital showed the peak of Se (0) at 54.58 eV, indicating that the oxidation state of selenium in Se-NPs was zero. Therefore, XPS analysis confirmed the foundation of Se-NPs on the printed wool fabric in Se (0) state [37].

Functional Properties of Se-NPs Printed Fabrics

Antimicrobial Activity

Antimicrobial activity of blank and Se-NPs printed wool fabrics towards different antimicrobial substance activity was determined in terms of zone of inhibition formed into agar media. The Se-NPs zones of inhibition against to G+ve (*S. aureus & Bacillus cereus*), G-ve (*E. coli*) and Yeast (*Candida utilis*) were measured in diameter (mm) for all organisms and the results were presented in Table 2. The blank wool fabric showed negligible antimicrobial properties, whereas the Se-NPs printed wool showed significant antimicrobial activity which increased by increasing the concentration of Se-NPs against the selected pathogenic strains. The high antimicrobial activity of Se-NPs may be attributed to Se-NPs large surface area that enhances better contact with microorganisms [38]. Moreover, Se-NPs act as an effective antimicrobial agent. On the other hand, Adomaviciute *et al.* revealed that PVP at the concentration of 8 % did not have any antimicrobial activity on *S. aureus*, *B. cereus*, *E. coli*, and *Candida* [39]. Since PVP concentration used in Se-NPs synthesis did not exceed 1.5 % in the current study, antimicrobial activity mainly corresponded to Se-NPs.

UV-Protection Properties

The UV-blocking properties of the printed wool fabrics

Table 2. Antimicrobial activity of Se-NPs printed wool fabric

Se-NPs conc.	Antimicrobial activity (ZI mm)			
	G+ve		G-ve	Yeast
	S. aureus	*B. cereus*	*E. coli*	*Candida utilis*
Blank wool	0	0	0	0
5 mM	18	16	14	20
12.5 mM	20	18	16	23
25 mM	23	21	18	25
37.5 mM	25	23	20	28
50 mM	27	26	23	30

ZI (zone of inhibitions).

Table 3. UV-protection properties of Se-NPs printed wool fabrics

Se-NPs conc.	UV-A Transmittance	UV-B Transmittance	UPF
Blank wool	10.43	1.72	33.46
5 mM	1.51	1.07	92.13
12.5 mM	1.46	0.83	115.6
25 mM	1.21	0.36	199.6
37.5 mM	0.59	0.42	224.15
50 mM	0.54	0.32	291.13

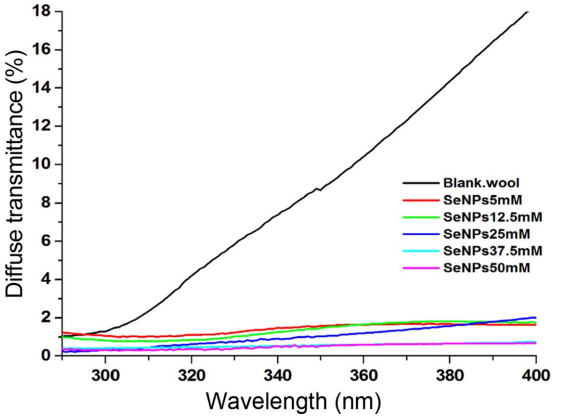

Figure 8. UV transmission through blank and Se-NPs printed wool fabrics.

Table 4. Cytotoxicity and IC_{50} of synthesized Se-NPs

Se-NPs conc. (μmol/m*l*)	Toxicity %	IC_{50} (μmol/m*l*)
0.195	1.17	
0.39	9.39	
0.781	52.58	
1.562	74.53	1.014
3.125	86.85	
6.25	89.79	
12.5	92.61	
25	94.13	

with Se-NPs were evaluated using UV light transmittance values plotted in Figure 8. The average values of transmittance in UVA (315-400 nm) and UVB (280-315 nm) regions of the wool fabrics were decreased obviously after printing with Se-NPs, which indicated a noticeable improvement in the ability of Se-NPs to act as UV-blocking of wool fabric. UV protection factor (UPF), which indicated the efficiency of the fabric in blocking solar UV radiation, was calculated from transmission data shown in Table 3. UPF value of blank fabric was observed to be 33.46 (Table 3). As shown in Table 3, printing with Se-NPs increased the UPF value of wool fabrics from 33.46 up to 291, which provided the printed fabrics with a rating of excellent in UV protection.

Testing

Cytotoxicity of Synthesized Se-NPs

Cytotoxicity of Se-NPs was evaluated using MTT assay on human cells (HFB_4). MTT is a tetrazolium salt which can be reduced to formazan by reducing enzyme found just in metabolically active cells [40]. Obtained results illustrated that no remarkable cytotoxicity was observed at a concentration of less than 0.195 μmol/m*l*. However, Se-NPs cytotoxicity increased gradually from 1.17 to 94.13 % with the increase in Se-NPs concentration from 0.195 to 25 μmol/m*l* as shown in Table 4, while IC_{50} of prepared Se-NPs was 1.014 μmol/m*l* (80.07 μg/m*l*).

Morphological changes such as cell shrinkage, nuclear condensation, and fragmentation are indicators for cytotoxicity

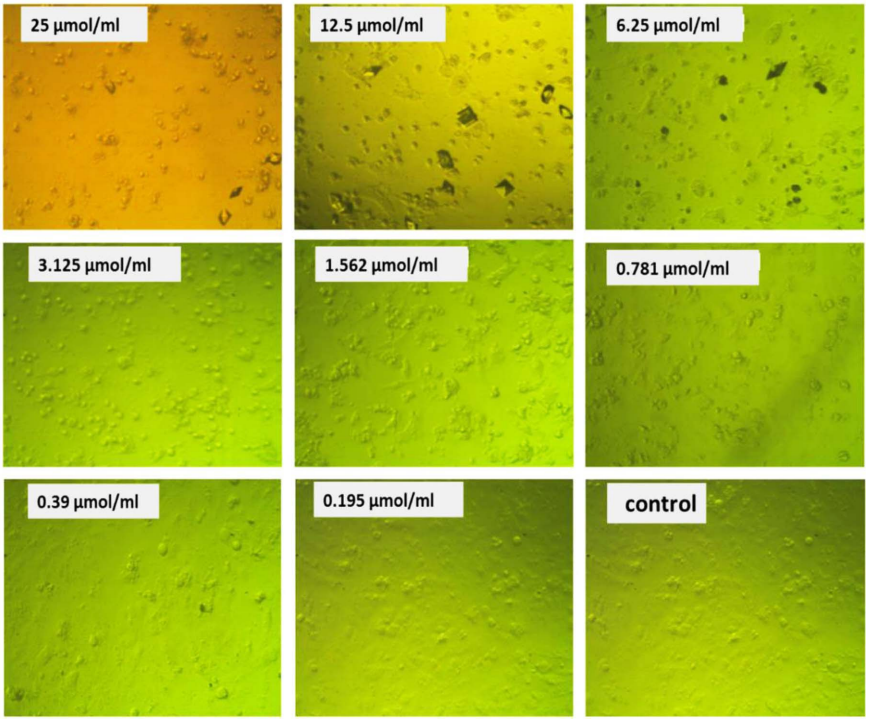

Figure 9. Effect of Se-NPs at different concentrations on HFB_4 cells viability.

[41]. They are noticed for the human normal melanocyte cells (HFB_4) and increased gradually with the increase in Se-NPs concentrations from 0.195 to 25 μmol/m*l* as displayed in Figure 9. HFB_4 cells lost their typical shape (control) and the cell density was decreased as a result of the increase in Se-NPs concentration.

Se-NPs had a lower cytotoxicity on normal human cells in comparison with several nanoparticles such as Ag-NPs. Paknejadi *et al.* studied the Ag-NPs cytotoxicity on normal human skin fibroblast cell line and found that Ag-NPs IC_{50} values were 30.64 and 14.98 μg/m*l* for 24 and 48 h of incubation, respectively [42], while Se-NPs showed IC_{50} value of 59.61 μg/m*l* on human dermal fibroblast cells [43].

Color Measurements

The colors of the printed wool fabrics arose from the characteristic SPR optical properties of synthesized Se-NPs. The printed wool fabrics displayed orange color varying in hue and tone depending on the concentrations of prepared Se-NPs as shown in Figure 10(a) and 10(b). Table 5 showed the colorimetric data for Se-NPs printed wool fabrics using CIELAB system in terms of L^*, a^*, and b^* demonstrating the effect of Se-NPs as a new colorant of wool fabrics.

Lightness (L^*) was decreased from 86.87 for the blank wool to 75.24 for the samples printed with 5 mM of synthesized Se-NPs, and then gradually decreased to 67.87 for the sample printed with 50 mM Se-NPs. This decrement in L^* was a result of coloration of wool fibers, which became more deeper by using higher concentration of Se-NPs.

At low levels of Se-NPs, the color of printed wool was light orange (Figure 10), which was also evident from the lower positive a^* and b^* values (Table 5). This value was gradually increased by increasing concentration of Se salt giving more reddish/yellowish (orange) tone to the printed fabrics. It was shown that the color saturation (C^*) could be controlled by varying the amount of hydrogen selenite and ascorbic acid. In general, the color became more saturated and darker (increase in C^* and decrease in L^*) with an increasing concentration of Se-NPs.

As expected, the color depth values expressed as *K/S* revealed an increasing trend shown in Figure 11. The progressive change in color appearance and *K/S* values supported the argument that the amount of Se-NPs deposited on wool surface via printing technique increased with the increase in concentration of both ascorbic acid and selenium salt.

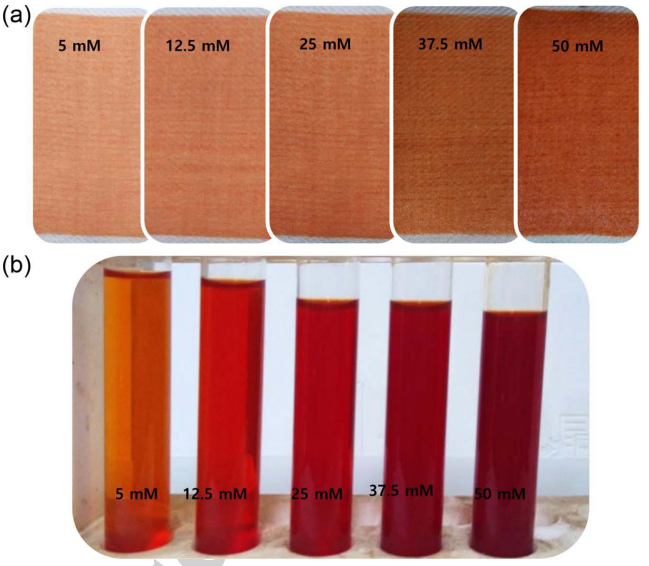

Figure 10. (a) Wool fabrics printed with Se-NPs of the same colors as in (b).

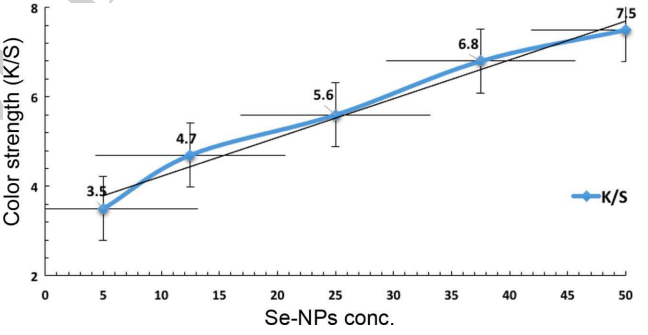

Figure 11. Effect of Se-NPs concentration on *K/S* of printed wool fabric.

Color Fastness Properties

The fading behavior of colored fabrics during washing, rubbing, and exposure to light are very important characteristics which affect its end use. Color fastness to washing, light, and rubbing were all evaluated for the Se-NPs printed fabrics

Table 5. Color characteristics and *K/S* values of Se-NPs printed fabric

Se-NPs conc.	*L**	*a**	*b**	*C**	*h*	*K/S*
Blank wool	86.87	0.96	12.33	12.37	85.56	1.1
5 mM	75.24	15.35	30.59	34.23	63.35	3.5
12.5 mM	71.48	17.58	33.99	35.63	60.43	4.7
25 mM	70.59	19.31	36.47	38.64	60.02	5.6
37.5 mM	63.42	25.38	39.29	49.06	53.22	6.8
50 mM	67.87	29.78	43.71	50.75	59.47	7.5

Table 6. Fastness properties of Se-NPs printed wool fabrics

Se-NPs conc.	Washing		Rubbing		Light
	St.	Alt.	Wet	Dry	
5 mM	5	4/5	4/5	5	4/5
12.5 mM	5	4/5	4/5	5	4/5
25 mM	5	4/5	4/5	5	4/5
37.5 mM	5	4/5	4/5	5	4/5
50 mM	5	4/5	4/5	5	4/5

Alt.: alteration, St.: staining on cotton.

and the results were listed in Table 6. All of printed wool fabrics have shown very good washing, rubbing (dry and wet), and light fastness results.

For all the printed samples, the alteration of color during washing showed very little color change (rating 4/5), and no staining was noticed on adjacent fabric (wool and cotton) (rating 5). The rubbing fastness generally showed very good rating. Dry rubbing fastness was observed to be a little better than the wet one, and the light fastness test showed very slight color fading rating of 4/5. This revealed the efficiency of the proposed procedure to figure out excellent coloration process without using any other chemicals (e.g. cross-linkers, binder, or coating materials).

Durability to Wash

For fabrics, good washing durability is an important and necessary factor for reuse. The washing durability test was indicated by AATCC Test Method 61(2A)-2009 after 10 laundering cycles, the Se-NPs printed wool fabrics were evaluated and the results were given in Table 7. The Se-NPs printed wool fabrics showed a slight decrease in their imparted functional properties, i.e. antimicrobial and UV-protection, but still high. The fastness properties and the color strength (*K/S*) of the obtained Se-NPs wool prints were still high even after 10 laundering cycles. It means that Se-NPs were still loaded and fixed onto simultaneously functional printed fabric surface.

Conclusion

A novel approach for upgrading the antimicrobial, UV-protection, and coloration characteristics of wool fabrics using colloidal solution of Se-NPs as a new functional colorant was investigated for the first time. The obtained results revealed that the printed wool fabrics have a stable bright color ranging from light orange gradually to dark orange with the concentration of synthesized Se-NPs with additional functionalities. The Se-NPs printed wool exhibited outstanding fastness properties and antimicrobial activity with excellent durability towards washing after 10 washing cycles. Moreover, the obtained prints effectively blocked the UV radiation providing excellent UV-protection.

Eventually, this unpretentious eco-friendly process assisted in producing multi-functionalities printed wool fabrics with brilliant colored by using nothing else but Se-NPs. The applicability of this method for other types of fabrics is being studied by our group in ongoing researches.

References

1. P. F. Tavcer, S. Kosir, and E. Csiszar, *Color. Technol*., **127**, 194 (2011).
2. K. Nemanja, S. Mladen, V. Gojko, G. Dragana, N. Dragoljub, M. Rastko, and P. Ivan, *Matéria (Rio J.),* **22**, 1 (2017).
3. N. A. G. Johnson and I. M. Russell in "Advances in Wool Technology", 1st ed. (I. M. Russell Ed.), Vol. 72, pp.61-83, Woodhead Publishing Ltd., England, 2009.
4. N. A. Ibrahim, M. H. Abo-Shosha, E. A. Allam, and E. M. El-Zairy, *Polym. Plast. Technol. Eng.*, **47**, 389 (2008).
5. C. R. Madhu and M. C. Patel, *Int. Res. J. Eng. Technol.*, **3**, 1236 (2016).
6. M. M. Marie, A. A. Salem, and E. M. R. El Zairy, *J. Text. Inst.*, **102**, 790 (2011).
7. M. Kanik and P. J. Hauser, *Color. Technol*., **118**, 300 (2002).
8. M. D. Teli, J. Sheikh, and P. Shastrakar, *J. Text. Sci. Eng.*, **4**, 39 (2014).

Table 7. Washing durability of imparted functional and color fastness characteristics of Se-NPs printed wool after 10 washing cycles

Se-NPs conc.	*K/S*	Fastness properties					Functional properties				
		Washing		Rubbing			ZI (mm.)				UPF
		St.	Alt.	Wet	Dry	Light	G+ve		G-ve	Yeast	
							S. aureus	*B. cereus*	*E .coli*	*Candida utilis*	
5 mM	3.2	5	4/5	4/5	5	4/5	16	14	12	18	90.42
12.5 mM	4.5	5	4/5	4/5	5	4/5	17	15	14	21	110.2
25 mM	5.5	5	4/5	4/5	5	4/5	20	18	16	23	195.3
37.5 mM	6.7	5	4/5	4/5	5	4/5	22	21	17	26	220.2
50 mM	7.3	5	4/5	4/5	5	4/5	24	23	20	28	288.5

Alt.: alteration, St.: staining on cotton, ZI (zone of inhibitions).

9. M. Rekaby, D. H. Shabaan, and H. A. Abdel-Ghany, *Int. J. Pharm. Sci. Rev. Res*., **40**, 142 (2016).
10. Sh. V. Singh and M. C. Purohit, *Indian J. Fiber Text.*, **39**, 97 (2014).
11. A. K. Samanta, P. Samanta, and D. Singhee, *Curr. Trends Fashion Technol. Text. Eng*., **2**, 69 (2018).
12. N. A. Ibahim, B. M. Eid, E. Abd El-Aziz, and T. M. Abou Elmaaty, *Carbohydr. Polym.*, **97**, 537 (2013).
13. N. A. Ibahim, B. M. Eid, T. M. Abou Elmaaty, and E. Abd El-Aziz, *Carbohydr. Polym*., **94**, 612 (2013).
14. N. A. Ibahim, T. M. Abou Elmaaty, B. M. Eid, and E. Abd El-Aziz, *Carbohydr. Polym*., **95**, 379 (2013).
15. N. A. Ibahim, E. Abd El-Aziz, B. M. Eid, and T. M. Abou Elmaaty, *J. Text. Inst.*, **107**, 1022 (2015).
16. M. Rehan, H. M. Mashaly, S. Mowafi, A. Abou El-Kheir, and H. E. Emam, *Dyes Pigm*., **118**, 9 (2015).
17. J. H. Johnston and K. A. Lucas, *Gold Bull.*, **44**, 85 (2011).
18. A. B. Rezaie, M. Montazer, and M. M. Rad, *J. Clean. Prod*., **166**, 221 (2017).
19. B. Tang, J. Wang, Sh. Xu, T. Afrn, J. Tao, W. Xu, L. Sun, and X. Wang, *Chem. Eng. J*., **185**, 366 (2012).
20. X. Lin, F. Zou, X. Chen, and B. Tang, *Mater. Sci. Eng*., **231**, 12077 (2017).
21. A. Jafari-Kiyan, L. Karimi, and A. avodiroknabadi, *Cellulose*, **24**, 3083 (2017).
22. T. Abou Elmaaty, Kh. El-Nagare, S. Raouf, Kh. Abdelfattah, S. El-Kadi, and E. Abdelaziz, *RSC Adv*., **8**, 25546 (2018).
23. K. Bai, B. Hong, J. He, Z. Hong, and R. Tan, *Int. J. Nanomed.,* **12**, 4527 (2017).
24. J. Yip, L. Liu, K. Wong, P. H. M. Leung, Ch. M. Yuen, and M. Cheung, *J. Appl. Polym. Sci*., **131**, 40728 (2014).
25. Ch. Ramamurthy, K. S. Sampath, P. Arunkumar, M. S. Kumar, V. Sujatha, K. Premkumar, and C. Thirunavukkarasu, *Bioprocess Biosyst. Eng*., **36**, 1131 (2013).
26. S. A. Wadhwani, M. Gorain, P. Banerjee, U. U. Shedbalkar, R. Singh, G. C. Kundu, and B. A. Chopade, *Int. J. Nanomed.*, **12**, 6841 (2017).
27. M. Kapur, K. Soni, and K. Kohli, *Adv. Tech. Biol. Med*., **5**, 2379 (2017).
28. S. Malhotra, N. Jha, and K. Desai, *Int. J. Nanotechnol. Appl*., **4**, 7 (2014).
29. AATCC Test Method 147-2004, **85**, NC 27709, USA, 2010.
30. T. Mosmann, *J. Immunol. Methods*, **65**, 55 (1983).
31. AATCC Test Method 61(1A)-2009, **85**, NC 27709, USA, 2010.
32. AATCC Test Method 8-2007, **85**, NC 27709, USA, 2010.
33. AATCC Test Method 16-2004, **85**, NC 27709, USA, 2010.
34. AATCC Test Method 61(2A)-2009, **85**, NC 27709, USA, 2010.
35. T. Satgurunathan, P. S. Bhavan, and S. Komathi, *Res. J. Chem. Environ*., **21**, 1 (2017).
36. R. Kirupagaran, A. Saritha and S. Bhuvaneswari, *J. Nano Technol*., **2**, 224 (2016).
37. K. Bai, B. Hong, J. He, Z. Hong and R. Tan, *Int. J. Nanomed.*, **12**, 4527 (2017).
38. D. M. Cruz, G. Mi, and T. J. Webster, *Biomed. Mater. Res*., **106**, 1400 (2018).
39. E. Adomavičiūtė, S. Stanys, M. Žilius, V. Juškaitė, A. Pavilonis, and V. Briedis, *Biomed. Res. Int*., **2016**, 11 (2016).
40. M. I. Sabela, T. Makhanya, S. Kanchi, M. Shahbaaz, D. Idress, and K. Bisetty, *J. Photochem. Photobiol. B*, **178**, 560 (2018).
41. M. Firdhouse and P. Lalitha, *Prog. Biomater*., **4**, 113 (2015).
42. M. Paknejadi, M. Bayat, M. Salimi, and V. Razavi, *Iran. Red Crescent Med. J.,* **20**, 10 (2018).
43. C. E. Hassan and T. J. Webster, *Int. J. Nanomed.*, **11**, 3641 (2016).